Entanglement of distant flux qubits mediated by non-classical electromagnetic field

2008 J. Phys.: Condens. Matter 20 275219

(http://iopscience.iop.org/0953-8984/20/27/275219)

J. Phys.: Condens. Matter **20** (2008) 275219 (7pp) doi:10.1088/0953-8984/20/27/275219

Entanglement of distant flux qubits mediated by non-classical electromagnetic field

E Zipper[1], M Kurpas[1], J Dajka[1] and M Kuś[2]

[1] Institute of Physics, University of Silesia, Ulica Uniwersytecka 4, 40-007 Katowice, Poland
[2] Center for Theoretical Physics, Polish Academy of Sciences, Aleja Lotników 32/46, 02-668 Warszawa, Poland

E-mail: mkurpas@us.edu.pl

Received 28 March 2008
Published 4 June 2008
Online at stacks.iop.org/JPhysCM/20/275219

Abstract
The mechanism for entanglement of two flux qubits each interacting with a single mode electromagnetic field is discussed. By performing a Bell state measurement (BSM) on photons we find the two qubits in an entangled state depending on the system parameters. We discuss the results for two initial states and take into consideration the influence of decoherence.

(Some figures in this article are in colour only in the electronic version)

1. Introduction

Entanglement is one of the most fundamental features of quantum mechanics. Besides its fascinating conceptual aspect it also plays an important role in quantum information science because entanglement of qubits is the essential requirement for quantum computing. Various systems have been considered as qubits [1, 2]; among them the solid state ones seem to be very promising. In particular the superconducting flux qubit has been developed in a superconducting ring with a Josephson junction [3, 4]. The junction playing the role of the tunneling barrier can be replaced by a superconducting quantum wire which allows for quantum phase slip [5]. Recently a flux qubit based on a semiconducting quantum ring with a controllable barrier has been proposed [6]. In this context the problem of the entanglement of two (or more) solid state qubits is of great importance. It has been investigated for superconducting flux qubits interacting via the mutual inductance, via a connecting loop with a Josephson Junction and via an LC circuit [4, 7–9]. It was found [7] that entangled states do not decohere faster than the uncoupled states. This is remarkable considering the expectation that spatially extended entangled states could be very susceptible to decoherence.

In this paper we want to study the entanglement of distant flux qubits by swapping. The model considerations presented may be applied both to superconducting or semiconducting flux qubits. We investigate two independently evolving subsystems each composed of a qubit exposed to a single mode of quantized electromagnetic field (figure 1). Contrary to the previous studies, where the so called external approximation was used [10], in this paper we take into account the full qubit–field interaction.

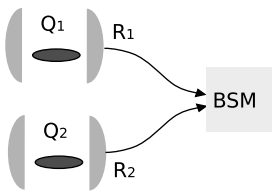

Figure 1. Entanglement swapping scheme.

Entanglement swapping was originally proposed for photons [11] and has been investigated both theoretically and experimentally [12, 13]. Recently this idea has been used to demonstrate the entanglement of two single atom quantum bits each spontaneously emitting a photon [14]. In our paper we use this idea to entangle solid state qubits which seem to be the most scalable and integrable [15]. The process of entanglement can be described in this case by the interaction Hamiltonian with controllable parameters. The use of solid state qubits instead of the atomic qubits described in [14] allows the building of systems operating at microwave rather than optical frequencies.

The scheme of entanglement swapping for the discussed system is presented in figure 1. Each qubit Q interacts with an

electromagnetic field mode R leading to an entangled qubit–field (QR) state. This effect has been observed in a series of experiments [16]. The two $(QR)_i$ ($i = 1, 2$) systems do not interact with each other and therefore the state of the whole system is a product state. If one then performs the Bell state measurement (BSM) on R_1 and R_2, the partner subsystems Q_1 and Q_2 will collapse to an entangled state although they have never physically interacted. To enhance the qubit–field interaction the qubits can be placed into the quantum cavity. The photons can escape from the cavity e.g. through a less reflecting mirror [15, 17]. To quantify the entanglement we calculate the negativity, and discuss the results for two different initial states.

In sections 2–4 we investigate the behavior over short timescales where the decoherence effects are negligible; the influence of decoherence is studied in section 5.

2. The qubit–cavity system

To show the idea we consider the rf-SQUID qubit [4] in the presence of static magnetic flux ϕ^{cl}. The Hamiltonian H_Q of such qubit can be written in a pseudo-spin notation

$$H_Q = -\tfrac{1}{2}B_z\sigma_z - \tfrac{1}{2}B_x\sigma_x. \tag{1}$$

We operate at $T \ll B_x/k_{\mathrm{B}}$ in order to neglect thermal fluctuations. The diagonal term B_z in (1) has the form

$$B_z = 2I_{\mathrm{c}}\sqrt{6(\beta_L - 1)}\left(\frac{\phi_0}{2} - \phi\right) \tag{2}$$

where $\beta_L = 2\pi L(I_{\mathrm{c}}/\phi_0) > 1$, $\phi = \phi^{\mathrm{cl}}$, I_{c} is the Josephson junction critical current, B_x is the tunneling energy between the two potential wells. Close to $\phi = \frac{1}{2}\phi_0$ ($\phi_0 = h/2e$) the ring is well described by the quantum superpositions of two opposite persistent current states.

At first we describe the process of entanglement of a qubit $Q_1(Q_2)$ with a single electromagnetic field mode $R_1(R_2)$. We model the electromagnetic field of the resonant cavity as an LC resonator described by H_R

$$H_R = \hbar\omega_R\left(a^\dagger a + \tfrac{1}{2}\right). \tag{3}$$

When the qubit is exposed to the quantized electromagnetic field the total flux $\phi = \phi^{\mathrm{cl}} + \phi^{\mathrm{q}}$, contains the quantum part

$$\phi^{\mathrm{q}} = \sqrt{\frac{\hbar}{2\omega_R C_R}}\left(a + a^+\right) \tag{4}$$

which leads to the qubit–field coupling. After some algebra we obtain

$$H_{QR} = \frac{\hbar\omega_Q}{2}\sigma_z + \hbar\omega_R\left(a^\dagger a + \tfrac{1}{2}\right) - \hbar\tilde{g}\left(a + a^\dagger\right)(\sigma_z\cos\theta - \sigma_x\sin\theta) \tag{5}$$

where ω_Q is the qubit frequency

$$\frac{\hbar\omega_Q}{2} = \frac{1}{2}\sqrt{\left(B_z^{\mathrm{cl}}\right)^2 + B_x^2}, \tag{6}$$

the 'mixing angle' θ [18] is

$$\theta = \tan^{-1}\frac{B_x}{B_z^{\mathrm{cl}}}, \tag{7}$$

and the coupling constant $\tilde{g}$ takes the form

$$\tilde{g} = I_{\mathrm{c}}\sqrt{\frac{3\,(\beta_L - 1)}{\hbar\omega_R C_R}}. \tag{8}$$

The above considerations can be equally well performed for a semiconducting flux qubit [6] with

$$B_z = 2I_0\left(\frac{\phi_0}{2} - \phi^{\mathrm{cl}}\right), \tag{9}$$

where I_0 is the amplitude of persistent current, $\phi_0 = h/e$, B_x describes the tunneling amplitude of an electron via a potential barrier.

Assuming realistic values of the parameters for superconducting qubit e.g. $\omega_R = 2\pi \cdot 50$ GHz, $I_{\mathrm{c}} = 0.5$ μA, we get $\tilde{g} = 0.2\omega_R$.

To discuss the qubit–field entanglement we assume that the coherent coupling overwhelms the dissipative processes (strong coupling regime). For creation and manipulation of entangled states, it is thus essential that both the cavity decoherence time T_R and the qubit decoherence time T_Q are much longer than the qubit–cavity interaction time $T_\Omega \sim \pi/\tilde{g} \sim 10^{-11}$ s. Recently a high quality cavities (quality factor $Q_{\mathrm{f}} \sim 10^5$–10^8) have been built [17, 18]. They have a photon storage time T_R in the range 0.3–300 μs. The estimated decoherence times T_Q of the considered qubits are of the order of a few microseconds (to be specific we assume $T_Q \sim 1$ μs [4]). In the next two sections we investigate the system at $t \ll T_Q, T_R$ allowing the entanglement to be obtained before the relaxation processes set in.

3. Entanglement swapping

The $(QR)_i$, $i = 1, 2$ system is described by a state vector $|\psi_{QR}(t)\rangle_i$, which at $t = 0$ is a direct product of the qubit and the cavity states:

$$\begin{aligned}\rho_{(QR)_i}(0) &= |\psi_{QR}(0)\rangle_{ii}\langle\psi_{QR}(0)|,\\ |\psi_{QR}(0)\rangle_i &= |\sigma n\rangle_i = |\sigma\rangle_i \otimes |n\rangle_i,\end{aligned} \tag{10}$$

where σ represents the qubit pseudo-spin states (g-ground, e-excited), $|n\rangle$ are the photon number eigenstates, forming the so called Fock basis, $n = 0, 1, 2, \ldots$.

The interaction of the qubit with the field leads, in general, to the entangled state

$$|\psi_{QR}(t)\rangle_i = \mathrm{e}^{-\frac{\mathrm{i}}{\hbar}H_{QR}t}|\psi_{QR}(0)\rangle_i. \tag{11}$$

As the two qubit-boson subsystems do not interact with each other their time evolved state remains separable:

$$\rho(t) = \rho_{(QR)_1}(t) \otimes \rho_{(QR)_2}(t). \tag{12}$$

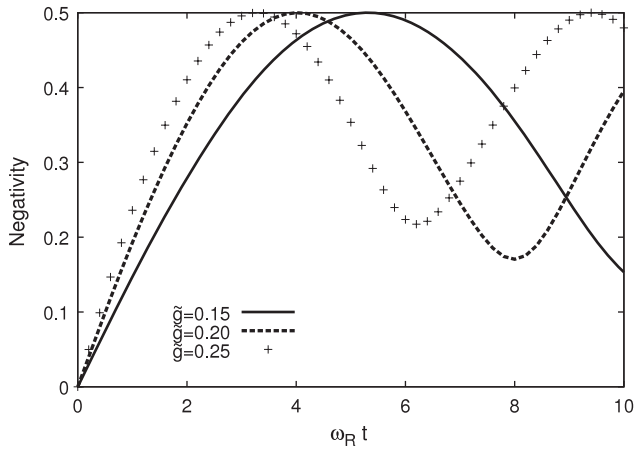

Figure 2. The qubit–field negativity for different values of $\tilde{g}$, $\theta = \pi/2$, initial state $|e0\rangle$ and $\omega_Q = \omega_R = 2\pi \cdot 50$ GHz.

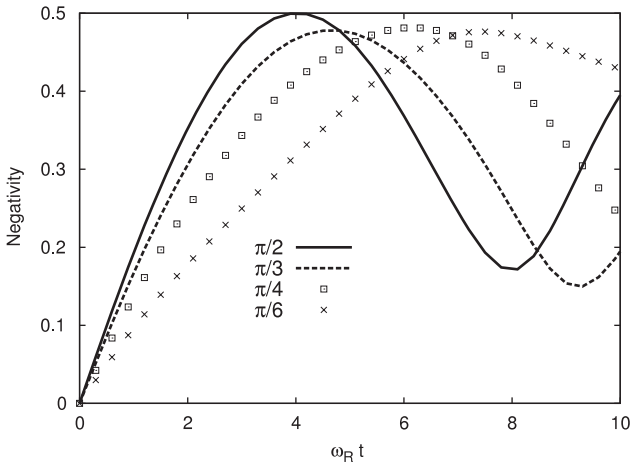

Figure 3. The qubit–field negativity for different values of θ, $\tilde{g} = 0.2$, initial state $|e0\rangle$, $\omega_Q = \omega_R = 2\pi \cdot 50$ GHz.

The time evolution of this composite is a product of two unitary evolutions of its constituents generated by the Hamiltonian (5) where

$$|\psi_{QR}(t)\rangle_1 = \sum_n [a_n(t)|gn\rangle_1 + b_n(t)|en\rangle_1] \tag{13}$$

$$|\psi_{QR}(t)\rangle_2 = \sum_n [\tilde{a}_n(t)|gn\rangle_2 + \tilde{b}_n(t)|en\rangle_2]. \tag{14}$$

The BSM is performed on electromagnetic field modes in the Fock basis (one photon with the vacuum) [12] and projects the formerly independent qubits onto an entangled state

$$\rho_{QQ}(t) = Tr_R\left(|B_R^1\rangle\langle B_R^1|\rho(t)\right), \tag{15}$$

where

$$|B_R^1\rangle = \frac{1}{\sqrt{2}}(|01\rangle - |10\rangle) \tag{16}$$

is one of the Bell states of the electromagnetic field modes, the trace Tr_R is taken with respect to photonic degrees of freedom.

After the BSM, the final qubit–qubit (QQ) state is of the form

$$\begin{aligned}|\psi_{QQ}\rangle = {} & [a_0(t)\tilde{a}_1(t) - a_1(t)\tilde{a}_0(t)]|gg\rangle \\ & + [a_0(t)\tilde{b}_1(t) - a_1(t)\tilde{b}_0(t)]|ge\rangle \\ & + [b_0(t)\tilde{a}_1(t) - b_1(t)\tilde{a}_0(t)]|eg\rangle \\ & + [b_0(t)\tilde{b}_1(t) - b_1(t)\tilde{b}_0(t)]|ee\rangle.\end{aligned} \tag{17}$$

We quantify the entanglement by the *negativity* [19] $N(\rho) = \max(0, -\sum_i \lambda_i)$, where λ_i are negative eigenvalues of the partially transposed [20] density matrix of the two qubits. For an entangled state, the negativity is positive reaching its maximal value $N = 0.5$ for maximally entangled pure state. It vanishes for disentangled states. Moreover, as it is an entanglement monotone it can be used to quantify the degree of entanglement. The use of negativity, instead of some entropic criteria as e.g. linear entropy, allows for the simultaneous treatment of the entanglement of pure and mixed states. Let us notice that in general (e.g. beyond the Jaynes–Cummings approximation) the qubit–resonator system evolves in an infinite-dimensional Hilbert space. It is known [21] that in high-dimensional systems the so-called PPT (positive with respect to partial transposition) entangled states can occur. They cannot be detected by the Peres criterion and negativity. In this paper we limit our attention to the NPT entangled states i.e those which are negative with respect to partial transposition.

4. Numerical results

We present results for entanglement of both qubit–field (N_i) and qubit–qubit (N_{QQ}) systems. As the calculations are numerical we are not limited to the weak coupling regime. In numerical calculations the Hilbert space of microwave modes is truncated at $n_{\max} = 10$. We test the validity of the truncation by controlling the traces of the matrices [22] to remain larger than 0.99.

There are many parameters affecting entanglement of qubits. To show the idea we restrict our considerations to selected examples and discuss the results for two initial states. In our model calculation we assume that both qubits are identical, the analysis can easily be extended further. In this paper we consider only the resonant case i.e. $\omega_{R_i} = \omega_{Q_i} \equiv \omega_R = 2\pi \cdot 50$ GHz. The values of $\tilde{g}_i$ are in the units of ω_R.

At first we assume the initial state to be

$$|\psi_{QR}(0)\rangle_1 \otimes |\psi_{QR}(0)\rangle_2 = |e0\rangle_1 \otimes |g1\rangle_2. \tag{18}$$

In figure 2 we show how the qubit–field negativity depends on the coupling strength $\tilde{g}$ and in figure 3 we show its behavior for different values of the mixing angle θ. Comparing these figures we see that both θ and $\tilde{g}$ influence the effective qubit–field interaction strength. The increase of $\tilde{g}$ causes an increase of the Rabi oscillation frequency and the entanglement arises faster than for weaker coupling. Similarly, bringing θ closer to $\pi/2$ increases the Rabi frequency. For $\theta = 0$ the QR entanglement disappears. In the following we assume $\theta = \pi/2$, which gives the strongest effective coupling with fixed $\tilde{g}$. In the upper panel of figure 4 the oscillating qubit–field negativities N_1 and N_2 reflect the varying degree of entanglement as a function of time. The differences in these two curves arise from different

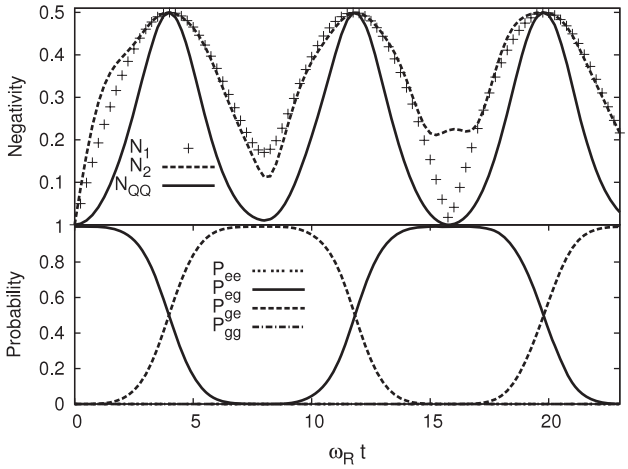

Figure 4. Negativities N_1 (crosses), N_2 (dashed line), N_{QQ} (solid line) and probabilities for finding the two qubits in different states after the BSM. The initial state $|e0\rangle_1 \otimes |g1\rangle_2$, coupling strength $\tilde{g}_i = 0.2$, $\theta_i = \pi/2$.

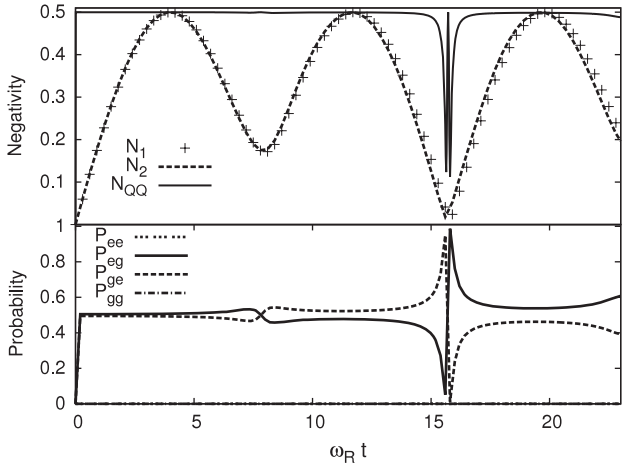

Figure 5. N_1 (crosses), N_2 (dashed line) and N_{QQ} (solid line) negativities (top) and probabilities (bottom) for the initial state (20), $\theta_i = \pi/2$ and small detuning $\tilde{g_1} = 0.2$, $\tilde{g_2} = 0.202$.

initial states for $(QR)_i$ systems ($|e0\rangle_1 \otimes |g1\rangle_2$). If we perform the BSM at a certain time t we obtain an entanglement of qubits (solid line) conditioned by the degree of entanglement of $(QR)_i$. In particular if we do the BSM in the time window in which the $(QR)_i$ subsystems are almost maximally entangled we obtain the maximally entangled qubits with $N_{QQ} \sim 0.5$. On the other hand if we perform the BSM in the time window where the $(QR)_i$ subsystems are weakly entangled the QQ entanglement is vanishingly small.

We emphasize that the 'time' in the figures is either the physical time of the quantum evolution of the QR system or the time, called the 'BSM time', at which the BSM was performed.

The bottom parts of figures 4 and 5 show the probabilities of finding the qubits in $|ee\rangle$, $|eg\rangle$, $|ge\rangle$ and $|gg\rangle$ states (e.g. $P_{\rm eg} = |\langle eg|\psi_{QQ}(t)\rangle|^2$). We see that the final state belongs to the subspace spanned by $|eg\rangle$ and $|ge\rangle$. This is because of the value of $\theta_i = \pi/2$ and the chosen projection operator. For such a θ the interaction term in (5) reduces to the form $\tilde{g}(a^\dagger + a)\sigma_x$ that excites only $|en\rangle$ with n even and $|gm\rangle$ with m odd if we start from $|e0\rangle$ and $|g1\rangle$ initial states respectively. Then when the BSM is done the only nonzero elements, in equation (17), are $b_1\tilde{a}_0$ and $a_1\tilde{b}_0$. The relationship between the 'occupation probabilities' can be directly translated into the entanglement of the state: the more one of the probabilities dominates the other the less entangled is the state and when the probabilities $P_{\rm eg}$ and $P_{\rm ge}$ equal 0.5 the entanglement reaches its maximal value.

The decay rate of the QR system can be estimated as [18]

$$\frac{1}{T_{QR}} = \frac{1}{2}\left(\frac{1}{T_Q} + \frac{1}{T_R}\right). \tag{19}$$

Assuming a cavity with $Q_{\rm f} = 10^5$ we find $T_R \sim 0.3\ \mu$s and $T_{QR} \sim 0.5\ \mu$s. For a cavity with $Q_{\rm f} = 10^6$ we get $T_R \sim 3\ \mu$s and $T_{QR} \sim 1.5\ \mu$s. The decoherence time of the QQ entangled state is accordingly $T_{QQ} \sim T_Q \sim 1\ \mu$s. This estimation is in agreement with the experimental findings [7] that entangled states do not decohere faster than uncoupled systems.

For the initial state

$$|\psi_{QR}(0)\rangle_1 \otimes |\psi_{QR}(0)\rangle_2 = |e0\rangle_1 \otimes |e0\rangle_2 \tag{20}$$

the situation looks different. The identity of the systems (the same parameters and initial states) leads to striking results. Whenever we perform the BSM we almost always (with some exceptions) obtain the maximally entangled qubit–qubit state. In order to show some subtleties we take the systems slightly detuned with $\tilde{g_1} = 0.2$, $\tilde{g_2} = 0.202$ and treat $\tilde{g_1} = \tilde{g_2} = 0.2$ as a limiting case. Because the two QR systems are almost identical, differing minutely in Rabi frequencies, they evolve to almost the same quantum states and even if the QR's are not strongly entangled the BSM gives nearly the same probabilities $P_{\rm eg} = P_{\rm ge} \sim 0.5$. In consequence, we get an almost maximally entangled QQ state for arbitrary BSM time, except for some moments (in figure 5 for $\omega_R t \sim 16$) at which the norm of the BSM output approaches zero and the above quantities become undefined. If the BSM were performed at these moments the entanglement would be unsuccessful. In the case $\tilde{g_1} = \tilde{g_2}$ the probabilities are always the same and the qubits get maximally entangled for each BSM time (see B line in figure 7) with the exceptions described above. Similar results we have obtained for the initial state $|g1\rangle_1 \otimes |g1\rangle_2$.

5. Decoherence

The design and construction of quantum devices is always limited by the influence of environment. Here, instead of a rigorous treatment, developed e.g. for pure dephasing [23, 24], we apply the commonly used Markovian approximation [25] and model the reduced dynamics of the QR system in terms of master equation generating complete positive dynamics [26]. Following [18] we assume that the effect of environment can be included in terms of two independent Lindblad terms:

$$\dot{\rho}(t) = [L_H - \tfrac{1}{2}L_1 - \tfrac{1}{2}L_2]\rho(t) \tag{21}$$

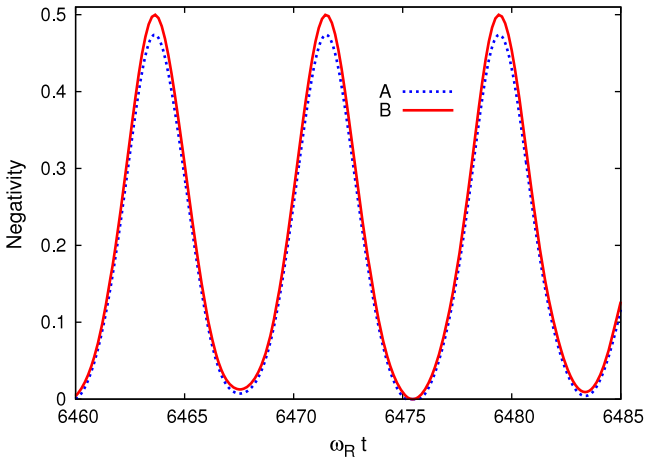

Figure 6. The QQ negativity with (A) and without (B) decoherence for the initial state (18). The parameters are $\theta_i = \pi/2$, $\tilde{g}_i = 0.2$, $T_{R_i} = 0.3\ \mu$s, $T_{Q_i} = 1\ \mu$s.

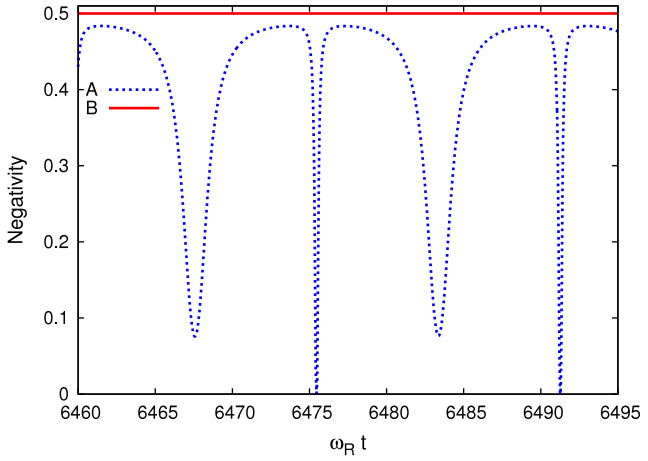

Figure 7. The QQ negativity with (A) and without (B) decoherence for the initial state (20). The parameters are as in figure 6.

where the 'conservative part' is given by

$$L_H(\cdot) = -\mathrm{i}[H_Q, \cdot] \tag{22}$$

whereas the 'Lindblad dissipators'

$$L_k(\cdot) = A_k^\dagger A_k(\cdot) + (\cdot)A_k^\dagger A_k - 2A_k(\cdot)A_k^\dagger, \qquad k = 1, 2 \tag{23}$$

are expressed in terms of creation and annihilation operators 'weighted' by suitable lifetimes $A_1 = a/\sqrt{T_R}$ and $A_2 = \sigma_-/\sqrt{T_Q}$. To be precise we assume $T_Q \sim 1\ \mu$s, $T_R \sim 0.3\ \mu$s. As the dynamics becomes non-unitary the system evolves, in general, to the mixed state. The BSM applied to the density operator of the mixed states is well defined physical operation of projection and reduction which can be shown to be completely positive (see appendix) and thus applicable to arbitrary ρ. In figure 6 we show the results of the master equation simulations of the negativity (the line labeled by A in figure 6) in comparison with the calculations which neglect decoherence (the line labeled by B) for the initial state (18). The periodicity with the decoherence included is conserved.

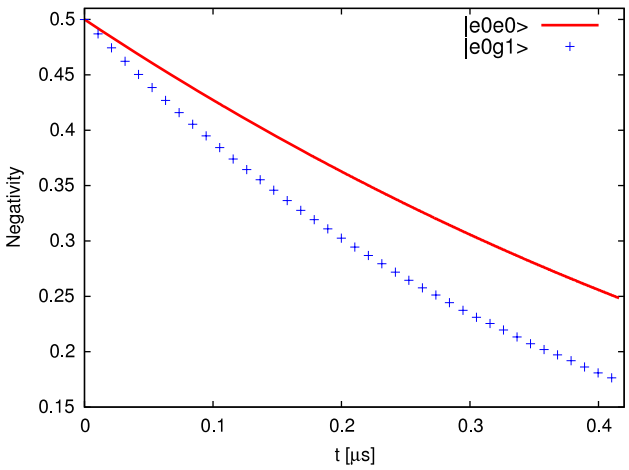

Figure 8. The amplitude of the qubit–qubit negativity plotted as a function of BSM time for two different initial states. The parameters are as in figure 6.

For better visibility we only present the results in a short time period. We see that decoherence slightly decreases the amplitude of the oscillations.

The influence of decoherence on the entanglement of the system starting from (20) (figure 7) is much more dramatic. In contrast to the non-dissipative case (B) the result of the BSM depends strongly on the BSM time and the character of the entanglement becomes quasi-periodic. In figure 8 we show the decrease of the amplitude of negativity as a function of time over a the larger timescale for both initial conditions. The decrease is faster for the initial state (18) in comparison with that for the initial state (20).

6. Conclusions

We investigated a mechanism for the creation of the entanglement of two qubits, each interacting with a single mode electromagnetic field coming from independent sources. This interaction leads to two independent entangled qubit–field states, and BSM performed on the electromagnetic field modes projects the qubits onto an entangled state. Thus we discussed the transfer of quantum information between systems having a different physical nature and defined in Hilbert spaces of different dimensions.

In the first part of the paper we have dealt with pure states which is justified to some extent by their estimated relatively long decoherence times. The systems discussed offer the advantage of reaching a strong coupling regime between light and matter. We have checked that the Jaynes–Cummings model, valid for weaker QR coupling [27], gives results in agreement with our calculations for $g \leqslant 0.03\omega_R$. Assuming reasonable values for the parameters we found that the strong coupling regime ($T_\Omega^{-1} \gg T_R^{-1}, T_Q^{-1}$) can be realized and coherent manipulation of qubits (especially with the quantum error correction technique) and maximally entangled qubit–qubit states is possible.

Analyzing the dynamics of the system in the presence of decoherence we found that the observation of coherent

phenomena and in particular the generation of highly entangled states is still possible.

It seems that entanglement of distant qubits by swapping can have some advantages over standard schemes of setting up entanglement that rely on generating entangled subsystems at a point and supplying them to distant areas. The qubits emerge entangled despite the fact that they have never interacted in the past and therefore they do not influence each other by disturbing the single qubit features. They can be at much larger distances as the scheme does not depend essentially on the distance between them. The degree of entanglement depends on the moment at which the BSM was performed. Verifying experimentally that two qubits are unambiguously entangled is a difficult task requiring sophisticated methods such as e.g. quantum state tomography [28]. The solid state qubits and their entanglement discussed in this paper can be scaled to a larger set of quantum bits [29]. It can be of interest in the study of the fundamental laws of quantum mechanics and can be useful in quantum information processing and quantum communication. It seems that the experimental realization of the presented model features may be performed with currently available technologies. Following [21], we hope that, sooner or later, 'what is predicted by quantum formalism must occur in the laboratory'.

Acknowledgments

JD thanks Marcin Mierzejewski for stimulating discussions concerning numerical methods applied in this paper. The work was supported by the Polish Ministry of Science and Higher Education under the grant N 202 131 32/3786 and by EU IP 'SCALA'.

Appendix

We will prove that the transformation described by (15) and (16) which was defined for pure states, also makes sense for an arbitrary mixed state of the two-qubit–field ($QRQR$) system, i.e. it is described by a completely positive operator transforming an arbitrary density matrix of the full system into a density matrix of the two-qubit (QQ) system. Although it is easy to understand on a purely physical basis (transformation consists of a measurement and a reduction to a subsystem), it is instructive to give an explicit proof of the statement. As a bonus we will easily find an explicit Kraus form of the transformation in question.

Let

$$\rho = \sum_{\substack{\mu k \nu l \\ \varsigma m \tau n}} \rho^{\mu k \nu l}_{\varsigma m \tau n} |\mu k \nu l\rangle\langle \varsigma m \tau n|, \tag{24}$$

where, cf (10),

$$|\mu k \nu l\rangle = |\mu\rangle_1 \otimes |k\rangle_1 \otimes |\nu\rangle_2 \otimes |l\rangle_2 = |\psi_{QR}\rangle_1 \otimes |\psi_{QR}\rangle_2 \tag{25}$$

for $\mu, \nu \in \{g, e\}$, $k, l \in \{0, 1, \ldots\}$ form a basis of pure states for the full system.

For the moment let us consider only the Jaynes–Cummings approximation where we take into account only the modes $|0\rangle$ and $|1\rangle$ of the electromagnetic field, hence all Latin indices in (24) and (25) take the values 0, 1 only. In this case density matrices of the $QRQR$ system act in the 16-dimensional complex space, $\mathcal{H}_1 = \mathbb{C}^{16}$, and as such form a subset of the 16×16-dimensional complex linear space. Analogously, density matrices of the QQ system, acting in the 4-dimensional complex space, $\mathcal{H}_2 = \mathbb{C}^4$, form a subset of the 4×4-complex space. The transformation (denoted in the following by Λ) described by (15) regarded on the whole 256-dimensional complex space transforms it into the 16-dimensional one. Straightforward calculations give

$$\Lambda(\rho) =: \sigma = \sum_{\substack{\mu, \nu \in \{g, e\} \\ \varsigma, \tau \in \{g, e\}}} \sigma^{\mu\nu}_{\varsigma\tau} |\mu\nu\rangle\langle\varsigma\tau|, \tag{26}$$

$$\sigma^{\mu\nu}_{\varsigma\tau} = \tfrac{1}{2}\left(\rho^{\mu 0 \nu 1}_{\varsigma 0 \tau 1} - \rho^{\mu 1 \nu 0}_{\varsigma 0 \tau 1} - \rho^{\mu 0 \nu 1}_{\varsigma 1 \tau 0} + \rho^{\mu 1 \nu 0}_{\varsigma 1 \tau 0}\right), \tag{27}$$

where $|\mu\nu\rangle := |\mu\rangle_1 \otimes |\nu\rangle_2$ form a basis of pure states of the QQ system. In the following we will need only

$$\begin{aligned}\Lambda\left(|\mu k \nu l\rangle\langle \varsigma m \tau n|\right) = \tfrac{1}{2}\big(&\delta_{0k}\delta_{1l}\delta_{0m}\delta_{1n} - \delta_{1k}\delta_{0l}\delta_{0m}\delta_{1n} \\ &- \delta_{0k}\delta_{1l}\delta_{1m}\delta_{0n} + \delta_{1k}\delta_{0l}\delta_{1m}\delta_{0n}\big)|\mu\nu\rangle\langle\varsigma\tau|.\end{aligned} \tag{28}$$

To check the complete positivity of Λ we use the Choi–Jamiolkowski isomorphism defined as [30]

$$\mathcal{J}(\Lambda) = (\Lambda \otimes \mathbb{I}_1)(P_+), \tag{29}$$

where $\mathbb{I}_1$ is the identity operator on the 256-dimensional space and P_+ is a maximally entangled state on the $\mathcal{H}_1 \otimes \mathcal{H}_1$ space

$$P_+ = |\Phi_+\rangle\langle\Phi_+|, \qquad |\Phi_+\rangle = \sum_{\mu k \nu l} |\mu k \nu l\rangle \otimes |\mu k \nu l\rangle. \tag{30}$$

According to the Choi theorem [31], Λ is completely positive if and only if $\mathcal{J}(\Lambda)$ is a positive definite operator. Applying (29) and (28) to (30) we get

$$\mathcal{J}(\Lambda) = |\Phi\rangle\langle\Phi|, \tag{31}$$

where

$$|\Phi\rangle = \frac{1}{\sqrt{2}} \sum_{\mu\nu} |\mu\nu\rangle \otimes \big(|\mu 0 \nu 1\rangle - |\mu 1 \nu 0\rangle\big). \tag{32}$$

Hence $\mathcal{J}(\Lambda)$ is a projection and as such a positive definite operator, consequently Λ is completely positive.

The obtained results allow us to write explicitly the so called Kraus form of Λ,

$$\Lambda(\rho) = \sum_n A_n \rho A_n^\dagger, \tag{33}$$

where A_n are $\dim \mathcal{H}_2 \times \dim \mathcal{H}_1 = 4 \times 16$ matrices. To this end [32] we have to perform the spectral decomposition of the positive definite operator $\mathcal{J}(\Lambda)$

$$\mathcal{J}(\Lambda) = \sum_\mu d_n |\chi'_n\rangle\langle\chi'_n|. \tag{34}$$

Since d_n are positive, we can rescale the eigenvectors

$$|\chi_n\rangle := \sqrt{d_n}|\chi'_n\rangle. \tag{35}$$

Now the operators A_n can be found in the form

$$A_n := \big(\mathbb{I}_2 \otimes \langle\Phi_+|\big)\big(|\chi_n\rangle \otimes \mathbb{I}_1\big), \tag{36}$$

where $\mathbb{I}_2$ is the identity on $\mathcal{H}_2$. The above formula should be properly understood. Observe that since $|\chi_n\rangle$ is an element of $\mathcal{H}_2 \otimes \mathcal{H}_1$, it has the form $|\chi_n\rangle = \sum_i |\phi_{n,i}\rangle \otimes |\xi_{n,i}\rangle$, where $|\phi_{n,i}\rangle \in \mathcal{H}_2$, $|\xi_{n,i}\rangle \in \mathcal{H}_1$, whereas $\langle\Phi_+| = \sum\langle\mu k\nu l| \otimes \langle\mu k\nu l|$. Hence

$$\begin{aligned} A_n &= \big(\mathbb{I}_2 \otimes \langle\Phi_+|\big)\,(|\chi_n\rangle \otimes \mathbb{I}_1) \\ &= \left(\mathbb{I}_2 \otimes \sum_{\mu k\nu l}\langle\mu k\nu l| \otimes \langle\mu k\nu l|\right)\left(\sum_i |\phi_{n,i}\rangle \otimes |\xi_{n,i}\rangle \otimes \mathbb{I}_1\right) \\ &= \sum_{i,\mu k\nu l} \langle\mu k\nu l|\xi_{n,i}\rangle\,|\phi_{n,i}\rangle\langle\mu k\nu l|. \end{aligned} \tag{37}$$

In our case $\mathcal{J}(\Lambda)$ has only one non-vanishing eigenvalue corresponding to the eigenvector $|\chi_1\rangle = |\Phi\rangle = \sum_{\mu\nu} |\phi_{1,\mu\nu}\rangle \otimes |\xi_{1,\mu\nu}\rangle$. Hence $|\phi_{1,\mu\nu}\rangle = |\mu\nu\rangle$ and $|\xi_{1,\mu\nu}\rangle = (|\mu 0\nu 1\rangle - |\mu 1\nu 0\rangle)/\sqrt{2}$. Using (32) and (37) we finally obtain:

$$A = \frac{1}{\sqrt{2}} \sum_{\mu\nu} \big(|\mu\nu\rangle\langle\mu 0\nu 1| - |\mu\nu\rangle\langle\mu 1\nu 0|\big). \tag{38}$$

A short calculation shows that indeed, cf (26),

$$\Lambda(\rho) = A\rho A^\dagger. \tag{39}$$

The calculations do not change considerably if we go beyond the Jaynes–Cummings approximation, by taking into account arbitrary finite numbers of photons in each cavity. In fact, in this case, the only difference consists of extending all summations over the number of photons from the two terms corresponding to 0 and 1 to the desired numbers of cavity excitations which we would like to include. The final results (38) and (39) remain unaltered. The situation is more subtle if we want to take into account the infinite number of possible photonic excitations of the cavity modes. The corresponding cavity Hilbert space becomes now infinite-dimensional and a straightforward generalization of the Choi–Jamiołkowski isomorphism does not exist—one has to resort to slightly more involved procedures to investigate directly the complete positivity [33]. It is, however, not really needed in our case. As is easy to check, the final result (38), (39) is also correct in the infinite-dimensional setting.

References

[1] Raimond J M, Brune M and Haroche S 2001 *Rev. Mod. Phys.* **73** 565
[2] Nakamura Y, Pashkin Yu A and Tsai J S 1999 *Nature* **398** 786
[3] Mooij J E, Orlando T P, Levitov L S, Tian L, van der Wal C H and Lloyd S 1999 *Science* **285** 1036
[4] Migliore R and Messina A 2003 *Phys. Rev.* B **67** 134505
Migliore R and Messina A 2005 *Phys. Rev.* B **72** 214508
[5] Mooij J E and Harmans C J P 2005 *New J. Phys.* **7** 219
[6] Zipper E, Kurpas M, Szelag M, Dajka J and Szopa M 2006 *Phys. Rev.* B **74** 125426
[7] Berkeley A J *et al* 2003 *Science* **300** 5625
McDermott R *et al* 2005 *Science* **307** 1299
[8] Plourde B L T *et al* 2004 *Phys. Rev.* B **70** 140501
Izmalkov A *et al* 2004 *Phys. Rev. Lett.* **93** 037003
[9] Paternostro M, Falci G, Kim M and Palma G M 2004 *Phys. Rev.* B **69** 214502
[10] Dajka J, Szopa M, Vourdas A and Zipper E 2004 *Phys. Rev.* B **69** 043505
Dajka J, Vourdas A, Zhang S and Zipper E 2006 *J. Phys.: Condens. Matter* **18** 1376
[11] Zukowski M, Zeilinger A, Horne M A and Ekert A K 1993 *Phys. Rev. Lett.* **71** 4287
[12] de Riedmatten H, Markicic I, van Houwelingen J A W, Tittel W, Zbinden H and Gisin N 2005 *Phys. Rev.* A **71** 050302
[13] Pan J-W *et al* 1998 *Phys. Rev. Lett.* **80** 3891
Pan J-W *et al* 2001 *Phys. Rev. Lett.* **86** 4435
Sciarrino F, Lombardi E, Milani G and De Martini F 2002 *Phys. Rev.* A **66** 024309
[14] Moehring D L, Maunz P, Olmschenk S, Younge K C, Matsukevich D N, Duan L-M and Monroe C 2007 *Nature* **449** 68
[15] Barrett S D and Kok P 2005 *Phys. Rev.* A **71** 060310(R)
[16] Chiorescu I *et al* 2004 *Nature* **431** 159
Walraff A *et al* 2004 *Nature* **431** 162
[17] Raimond J M, Brune M and Haroche S 2001 *Rev. Mod. Phys.* **73** 565
[18] Blais A, Huang R, Wallraff A, Girvin S M and Schoelkopf R J 2004 *Phys. Rev.* A **69** 062320
[19] Vidal G and Werner R F 2002 *Phys. Rev.* A **65** 032314
[20] Peres A 1996 *Phys. Rev. Lett.* **77** 1413
[21] Horodecki R, Horodecki P, Horodecki M and Horodecki K 2007 *Preprint* quant-ph/0702225v2
[22] Migliore R, Konstadopoulou A, Vourdas A, Spiller T P and Messina A 2003 *Phys. Lett.* A **319** 67
[23] Łuczka J 1990 *Physica* A **167** 919
[24] Dajka J, Mierzejewski M and Łuczka J 2007 *J. Phys. A: Math. Theor.* **40** F879
[25] Gadiner C W and Zoller P 2000 *Quantum Noise* (Berlin: Springer)
[26] Alicki R and Lendi K 1987 *Quantum Dynamical Semigroups and Applications* (*Springer Lecture Notes in Physics*) (Berlin: Springer) p 286
[27] Sornborger A T, Cleland A N and Geller M R 2004 *Phys. Rev.* A **70** 052315
[28] Steffen M *et al* 2006 *Science* **313** 1423
[29] Bose S, Vedral V and Knight P L 1998 *Phys. Rev.* A **57** 822
[30] Jamiolkowski A 1972 *Rep. Math. Phys.* **3** 275278
[31] Choi M D 1975 *Linear Algebra Appl.* **10** 285290
[32] Arrighi P and Patricot C 2004 *Ann. Phys.* **311** 2652
[33] Grabowski J, Kuś M and Marmo G 2007 *Open Syst. Inf. Dyn.* **14** 355